Journal of Integrative Agriculture
2013, 12(8): 1316-1329

Available online at www.sciencedirect.com
ScienceDirect

August 2013

RESEARCH ARTICLE

Analysis of the Diurnal Pattern of Evaporative Fraction and Its Controlling Factors over Croplands in the Northern China

YANG Da-wen, CHEN He and LEI Hui-min

State Key Laboratory of Hydroscience and Engineering, Department of Hydraulic Engineering, Tsinghua University, Beijing 100084, P.R.China

Abstract

A key issue of applying remotely sensed data to estimate evapotranspiration (ET) for water management is extrapolating instantaneous latent heat flux (LE) at satellite over-passing time to daily ET total. At present, the most commonly used extrapolation methods have the same assumption that evaporative fraction (EF) can be treated as constant during daytime (so-called EF self-preservation). However, large errors are reported by many documents over various ecosystems with the same approach, which indicates that further analysis of the diurnal pattern of EF is still necessary. The aim of this study is to examine the diurnal pattern of EF under fair weather conditions, then to analyze the dependencies of EF to meteorological and plant factors. Long-term flux observations at four sites over semi-arid and semi-humid climate regions in the northern China are used to analyze the EF diurnal pattern. Results show that the EF self-preservation assumption no longer holds over growing seasons of crops. However, the ratio of reference ET to available energy is almost constant during the daytime, which implies the climate factors do not have much effect on the variability of EF. The analysis of diurnal pattern of air temperature, vapor pressure deficiency (VPD), and relative humidity (RH) confirms the assumption that ET diurnal pattern is mainly influenced by stomatal regulation.

Key words: evaporative fraction, daily evapotranspiration, meteorological factor, vegetation fraction, northern China

INTRODUCTION

Evapotranspiration (ET) is one of the most important components of energy and water balances in agricultural ecosystem (Burba and Verma 2005). Accurate ET estimation is of crucial importance for water resource management, especially over croplands in semi-arid and semi-humid climate, because agriculture consumes about 80% of the available water in the northern China (Yang *et al*. 2004). Remote sensing data can provide surface parameters of both continuous spatial coverage and acceptable recurrence interval of 1-2 d for polar-orbiting satellite and tens of minutes for geostationary platforms (Kustas *et al*. 2004), thus it becomes an effective approach in estimating ET at regional scale. Recently, remote sensing ET models proposed for estimating regional or global actual ET have an explosive growth (e.g., Bastiaanssen *et al*. 1998; Su 2002; Allen *et al*. 2007; Sànchez *et al*. 2008). However, one of the key issues of applying remote sensing data to estimate regional ET involves the scaling from instantaneous latent heat flux (LE) at satellite over-passing time (e.g., Landsat, 10:00 a.m.; ASTER, 11:30 a.m.; AVHRR, 14:00 p.m.) to daily ET total, because daily ET is usually required for agricultural water management. The most practical solution is extrapolating the instantaneous LE calculated from remote sens-

Received 17 October, 2012 Accepted 10 January, 2013
Correspondence CHEN He, Tel: +86-10-62782044, Fax: +86-10-62796971, E-mail: chenhe86@gmail.com

doi:10.1016/S2095-3119(13)60540-7

ing models to daily scale by a general and robust method (Hoedjes *et al*. 2008).

Many ET extrapolation approaches have been well documented, such as sine function method (Jackson *et al*. 1983; Zhang and Lemeur 1995), constant evaporative fraction method (Sugita and Brutsaert 1991), and constant reference ET fraction method (Allen *et al*. 2007), etc. Detailed instruction of scaling from instantaneous ET to daytime integrated value was presented by Li *et al*. (2009). Among those approaches, the most commonly accepted method is constant evaporative fraction (EF) method, which assumes the EF is constant during the daytime (so called self-preservation of EF). EF is define as the ratio between LE and the available energy (EF=LE/(R_n-G)), which is an important indicator of the surface hydrological history (Shuttleworth *et al*. 1989). Many experimental studies over various vegetation species verified the self-preservation of EF (Brutsaert and Sugita 1992; Crago 1996; Crago and Brutsaert 1996), and demonstrated the high correlation between EF in the midday and the whole daytime, despite some underestimation existed in the range of 5-10% (Sugita and Brutsaert 1991; Kustas *et al*. 1993; Nichols and Cuenca 1993). However, unacceptable large errors were reported by Stewart (1996) in estimating daily ET by constant EF method, and he concluded many variables controlling the EF diurnal pattern which needed further analyzed. To date, detailed analysis of EF diurnal pattern and its controlling factors have been extensively studied by models or by experiments. A typical concave-up shape for EF was reported by Lhomme and Elguero (1999), and the diurnal pattern of EF was demonstrated affected by complicated variables such as vegetation coverage, soil moisture, stomatal conductance, etc. (Suleiman and Crago 2004; Li *et al*. 2006; Gentine *et al*. 2007). However, most of the previous studies on EF were only able to study the diurnal EF pattern during a few days (no more than a season), or merely by scenario analyses based on a model; while a comprehensive understanding of the general pattern of diurnal EF needs a long term experiment and analysis over variant land covers and climates. Li *et al*. (2008) examined the pattern of vineyard EF by eddy covariance technique over the arid desert region of Northwest China and pointed out that further analysis and research of the EF diurnal pattern is still necessary in various agricultural lands in China.

The present study has two objectives of (1) examining the diurnal pattern of EF over typical croplands in the northern China and (2) analyzing the discrepancies of EF to meteorological parameters and plant physiology. We choose northern China as our study area because few studies of the EF diurnal pattern have been done in this area, which is the major grain production area and is facing severe water scarcity. To this end, long term observation of energy fluxes associated with meteorological parameters were carried out at four flux sites over different land covers and climates in the northern China. We first analyze the general pattern using the long term EF diurnal pattern at the four sites. Then we analyze the influence factors of EF by separating the factors into climate factors and plant factors.

RESULTS AND DISCUSSION

Hydrometeorological conditions of the four sites

Soil moisture availability and vegetation canopy condition are the two main dominant factors of EF (Gentine *et al*. 2007). Mean level of the soil water content (SWC) in region 1 is higher than that in region 2 (Fig. 1) because of the lack of precipitation and irrigation in region 2. The seasonal pattern of the SWC in region 1 is relatively gentle throughout the year, although most of the precipitation concentrated in the maize growing seasons (Fig. 1-A and B). This is mainly because the accommodation of irrigation during the wheat growing seasons, and owing to this, the SWC is generally higher than the moisture stress threshold (0.22 m^3 m^{-3}) during the crop growing seasons. In Weishan site, the interannual variation is rather small due to the adjustment of irrigation (Fig. 1-A), in spite of the drought year in 2006 (total precipitations of 274 mm). In Tongyu site however, acute variability of SWC is found, because the SWC is sensitive to precipitation (Fig. 1-C and D). The total precipitation of 2004 is only 182 mm, and the SWC is at a low level in both crop land and grass land all year round.

In region 1, the fractional coverage reaches its maximum at the vigorous vegetative seasons except for 2006

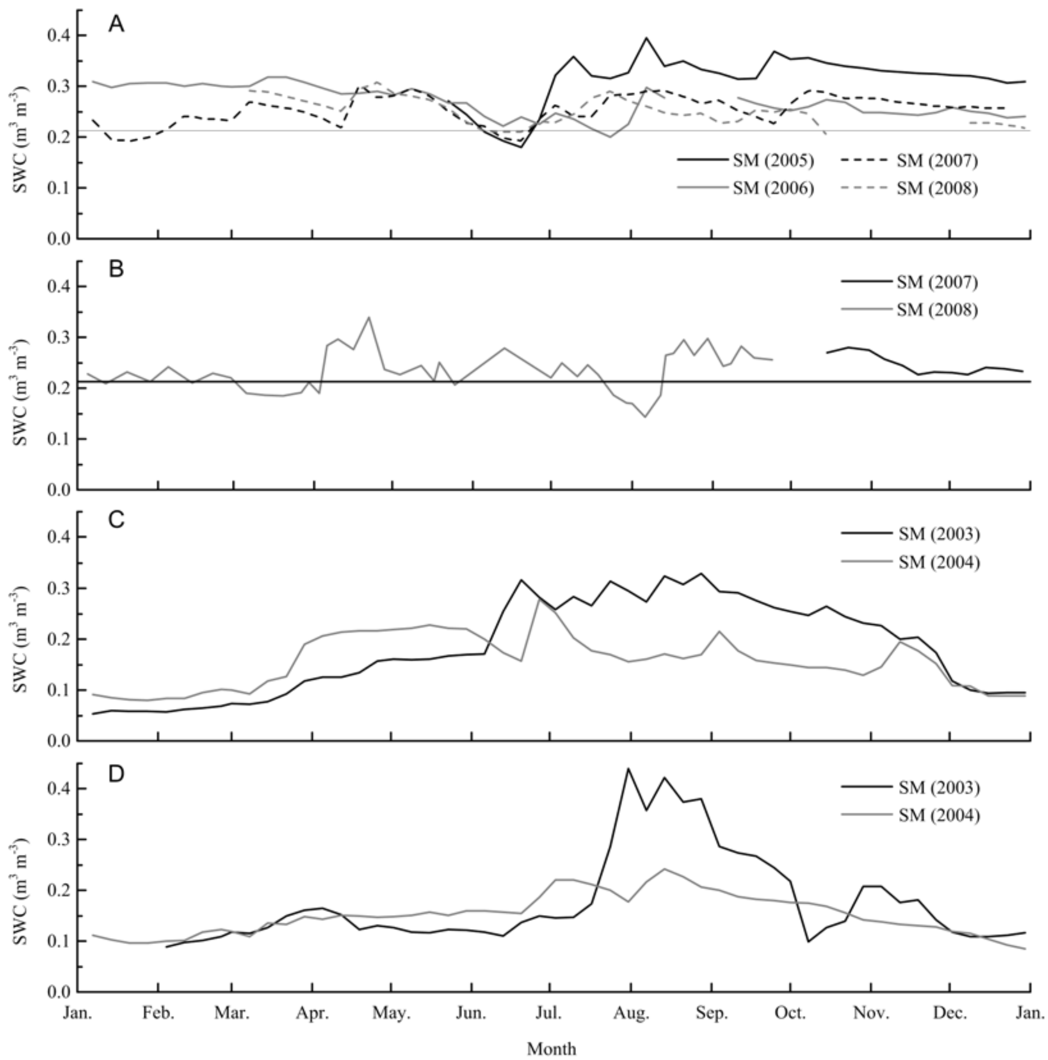

Fig. 1 Weekly averaged soil water content (SWC) at different sites. A, Weishan site (0-20 cm averaged). B, Luancheng site (0-40 cm averaged). C, Tongyu site on crop land (0-20 cm averaged). D, Tongyu site of grass land (0-10 cm averaged).

because of drought (Fig. 2-A and B). The trough appears in June, which is the crop rotation period between the wheat and maize seasons. The fractional coverage increases again in November because of the emergence of winter wheat, and then decreases when winter wheat goes to dormancy. In region 2, the fractional coverage is very low in the dry season (October to the following May) and even in wet season, the fractional coverage can hardly reach its maximum (Fig. 2-C and D). The inter-annual variation is dramatic, and in the year 2004, the maximum fractional coverage is merely 0.5 and 0.6 for cropland and grassland, respectively. Vegetation cover and soil moisture level greatly affect the ratio of soil evaporation to total evapotranspiration. In region 1, the transpiration during the vigorous vegetative months can take up 70% of the total ET (Liu *et al*. 2002). Thus in Tongyu site, we can come in to a conclusion that the ratio of soil evaporation to the total ET is larger than that in Weishan and Luancheng sites.

Diurnal pattern of measured EF

All the data in the four sites are used to examine the diurnal pattern of EF. Figs. 3 and 4 show the diurnal ensemble mean value of EF during the daytime in regions 1 and 2, respectively. In the vigorous vegetative season, EF presents an increasing pattern during daytime, despite some inter-annual change within these years. For example, between the turning-green stage

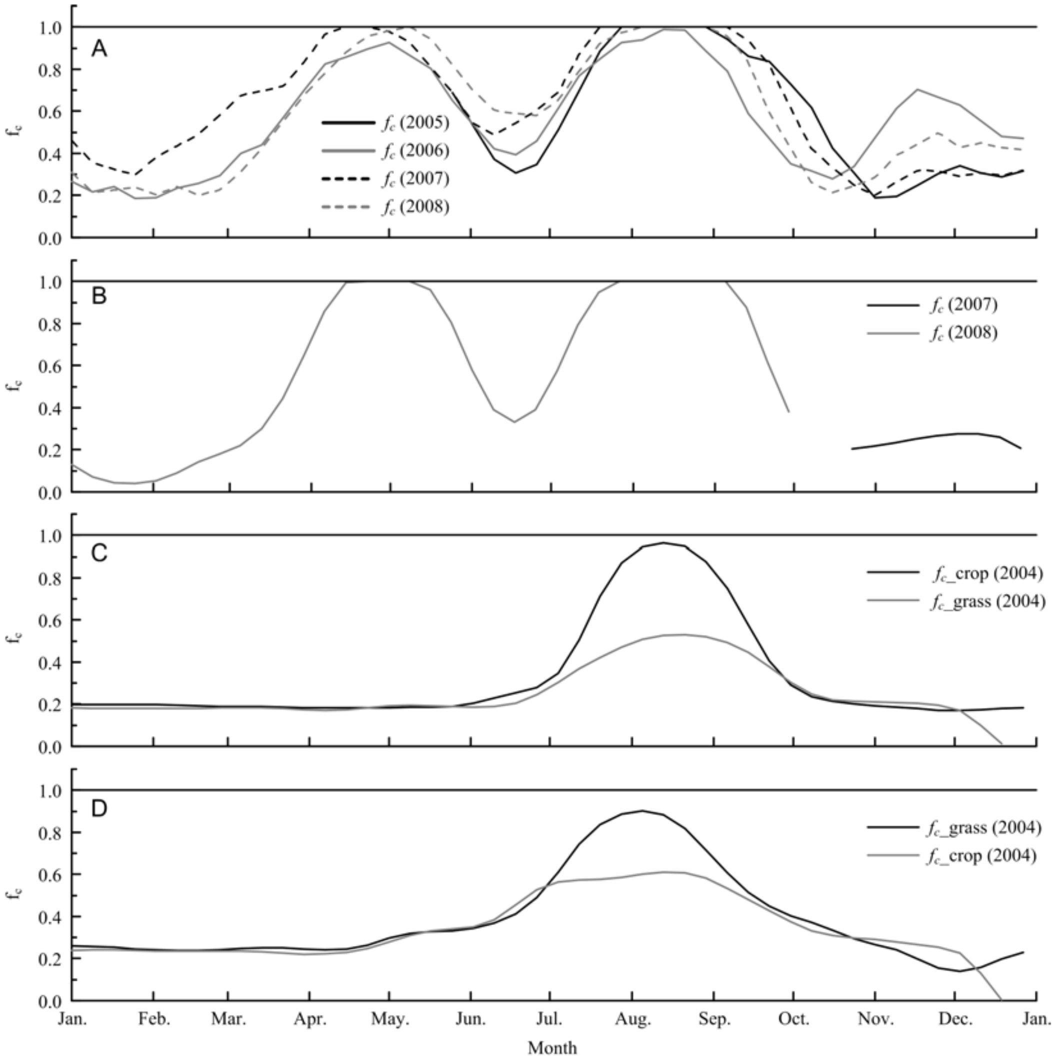

Fig. 2 Fractional coverage (f_c) of at different sites. A, Weishan site. B, Luancheng site. C, Tongyu site on crop land. D, Tongyu site of grass land.

to the harvest time of wheat growing season in region 1 (Fig. 3-C and E), the EF increased notably from sunrise to sunset in both sites. In these figures, the EF increases continuously during the day, except a decrease at the first hour after the sunrise which might be contributed to the unstable flux in the morning. Same pattern of EF is found in the whole maize growing season in the same region (Fig. 3-G-I), but the EF increases slowly at most of the day and then increases rapidly a few hours before sunset. In region 2, however, only in July and August does the EF pattern similar as what shows in region 1 (Fig. 4-G-H), which are the months with the most precipitation and thus the vegetation is the most vigorous. In the remaining three months of the growing season (Fig. 4-E, Fand I), the EF is nearly constant in the most time of the day and increases sharply in the late afternoon. Experiments of EF diurnal patterns are also made by other researchers over different landcover, but the increasing pattern of EF has not been reported. Caparrini *et al*. (2004) conducted a three months' experiment over a grass land and found out that the EF was nearly constant from 9:00 a.m. to 4:00 p.m. Chehbouni *et al*. (2008) measured daily pattern of EF over maize and wheat fields, but a typical concave-up shape for EF variation was found from the results. The different diurnal pattern of EF indicates that the reason is need to be explored.

On the other hand, the EF is nearly constant during

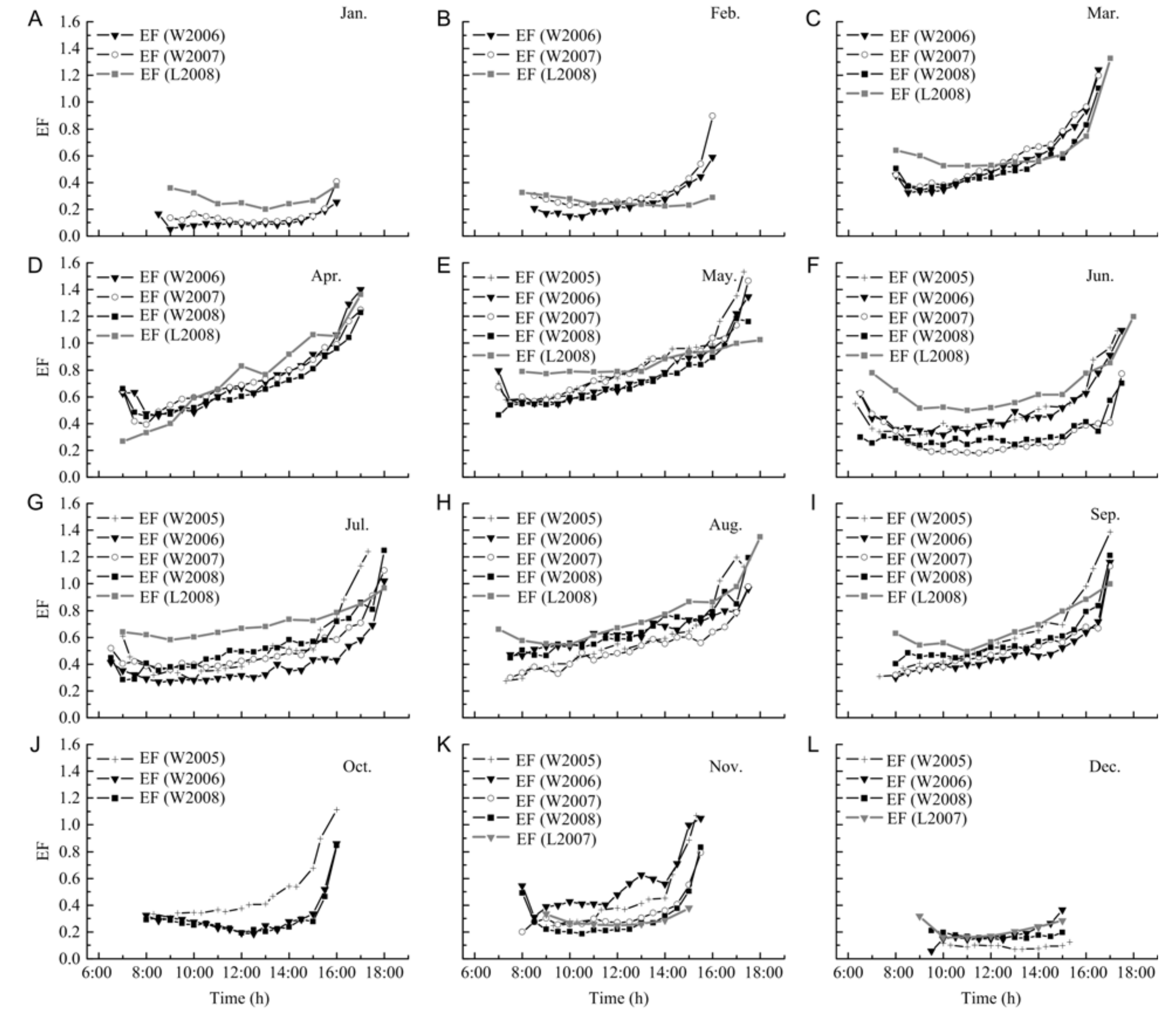

Fig. 3 Monthly mean value of EF diurnal pattern in region 1. W, Weishan site; L, Luancheng site.

near-peak radiation hours in the non-vegetation months over both regions. For example, in the December and the following January in region 1 (Fig. 3-A and L), and the dry seasons in region 2 (Fig. 4-A-D and J-L), the landcover is almost bare soil and the height of the plants is less than 5 cm, respectively. This result is similar to the former researchers, as Hoedjes *et al*. (2008) found that when the Bowen ratio is higher than 1.5 (i.e., EF lower than 0.4), the EF is relatively constant despite some variation, and attributed the reason to the dry weather conditions. Li *et al.* (2008) also reported the constant EF over a vineyard in the arid region. But in region 1 of the present experiments, the EF diurnal pattern is still relatively constant in June (i.e., the intermittent of the wheat and maize) when the weather is rather wet while the landcover is almost bare soil (Fig. 4-F). Similar results were reported by Stewart (1996) over savannah and open forest in a semi-humid region. The diurnal EF increased prominent in the open forest but not so much in savannah, and the month-to-month variation in open forest was larger than that for savannah.

According to the result at the present experiment, two conclusions can be drawn. First, the magnitude of EF varies from site to site, and year to year, which reflects the influences of meteorological factors as mentioned in the former section. Second, the assumption of the self-conservation of EF during daytime hours is only valid under bare soil landcover condition, while

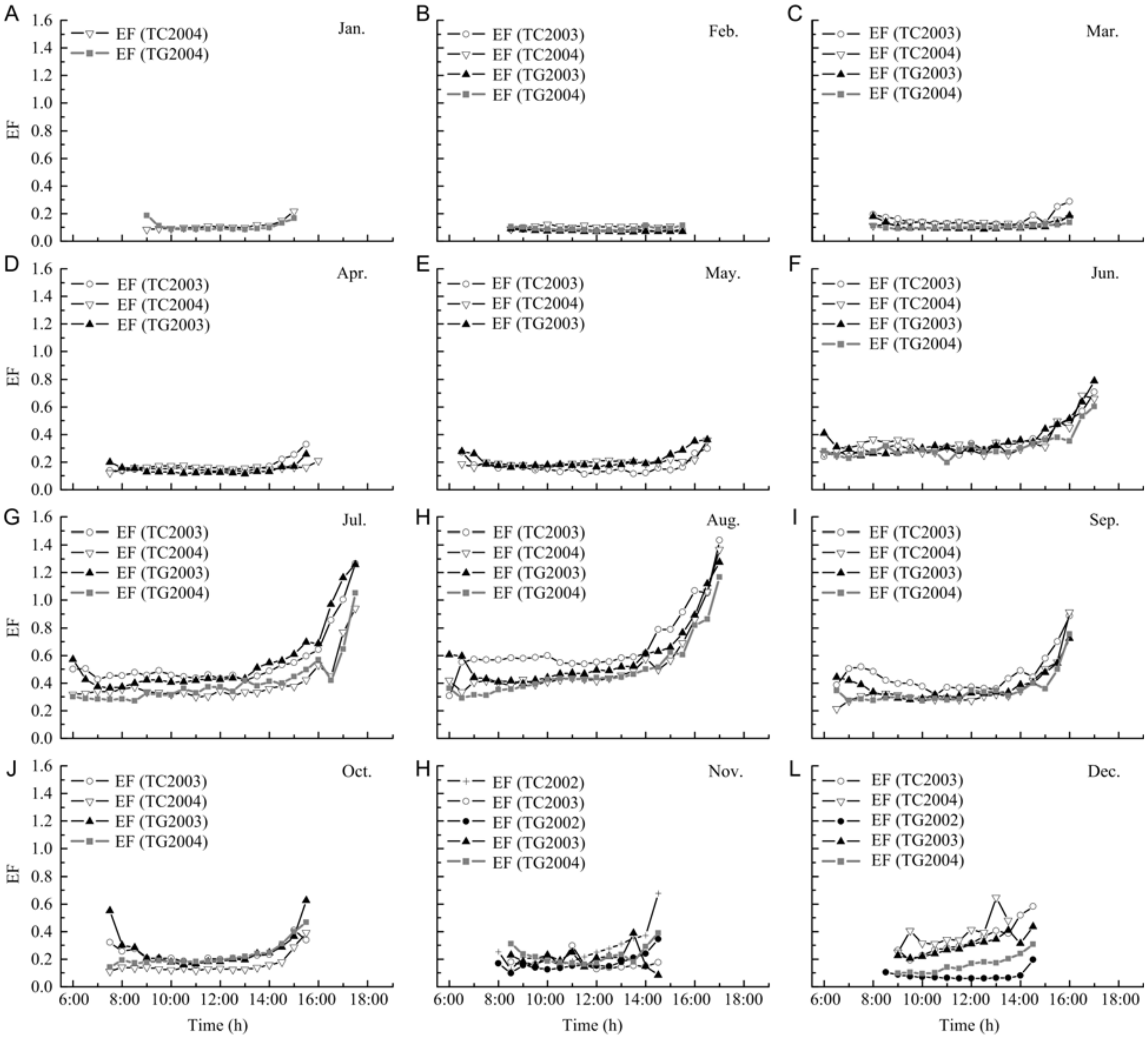

Fig. 4 Monthly mean value of EF diurnal pattern in region 2. TC, Tongyu crop land site; TG, Tongyu grass land site.

an increasing diurnal pattern is observed for vegetation landcover. Moreover, the more vigorously the vegetation grows, the sharper the EF diurnal shape is. Therefore, the approach of the self-preservation assumption to all surface conditions may induce large bias in extrapolating daily ET.

EF diurnal pattern dependencies

Figs. 5 and 6 show the ensemble mean value of diurnal pattern of ET_rF in region 1 and region 2, respectively. Same pattern is found in both of the two regions that the ET_rF is relatively constant during the daytime with a slightly increasing trend, though the magnitude varied from month to month. Compared with ET_rF diurnal pattern, the EF diurnal pattern has a similar pattern during non-vegetation cover seasons, because the stomatal regulation is rather weak due to the lack of vegetation. But the magnitude of EF is commonly lower than that of ET_r, as an aggregate result of the soil water stress and vegetation coverage, for the crop efficient K_c is mainly influenced by these two factors. In the vegetative season, however, the EF diurnal pattern is quite different from that of the ET_rF, and shows an obvious seasonal characteristic. For region 1, in the wheat and maize vigorous seasons (March-May, July-October),

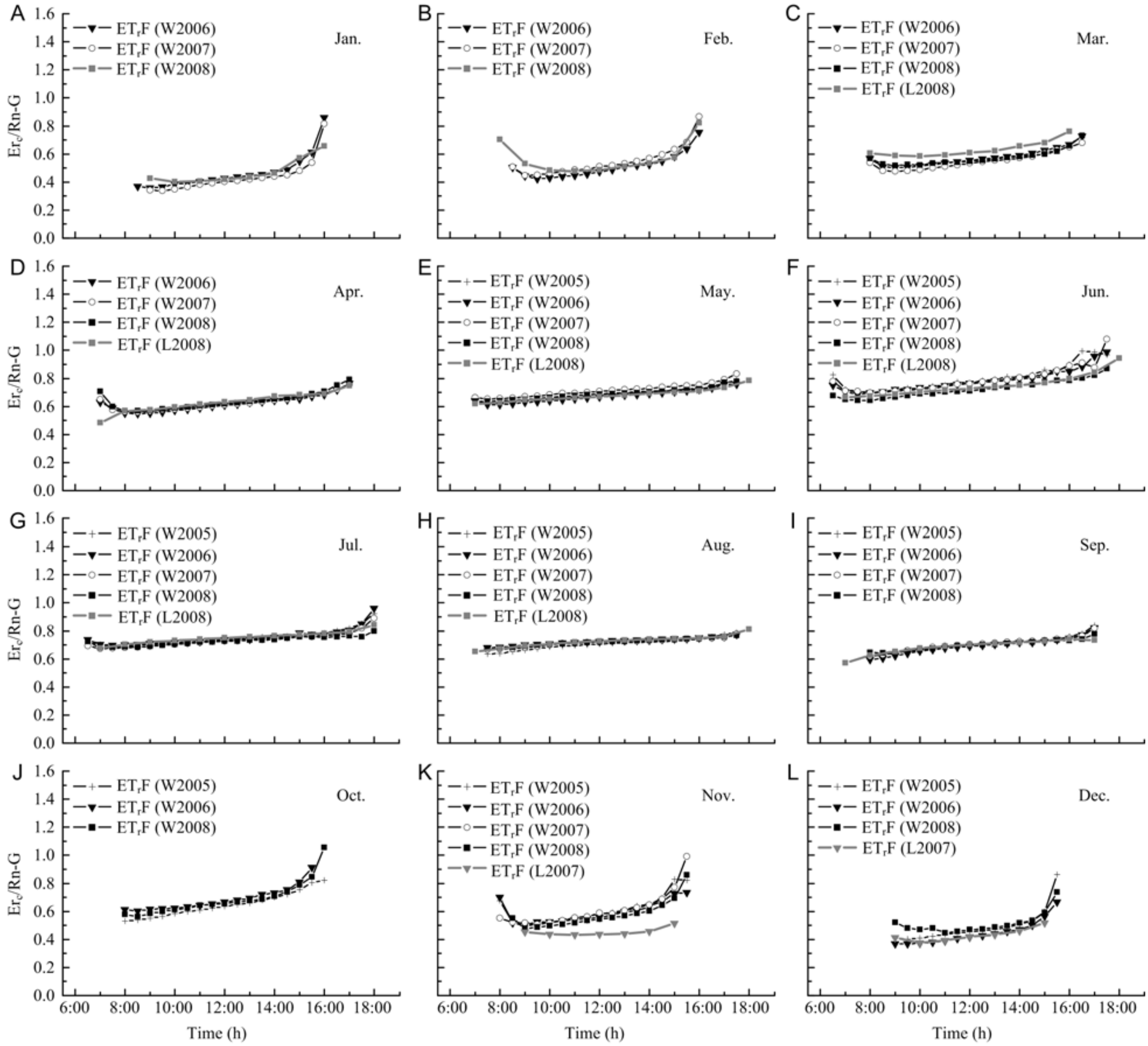

Fig. 5 Monthly mean value of the ratio of ET_rF diurnal pattern in region 1. W, Weishan site; L, Luancheng site.

the EF is smaller than ET_rF in the morning, and surpasses it around noon time. While in region 2, the EF can hardly catch up with ET_rF during the daytime, except the last few hours before sunset. The differences in the magnitude of EF in regions 1 and 2 show the differences in soil moisture content, that is to say, in region 2, the vegetation is more likely to suffer from the soil moisture stress, and the transpiration of the vegetation is inhibited. Trezza (2002) proposed the hypothesis that the relationship between actual ET and reference ET_r remained constant during the daytime, and validated the hypothesis over grassland and sugar beets land with a lysimeter. This approach was further applied by Allen *et al*. (2007) in the METRIC model. In the present study, however, the approach is adaptable in non-vegetation seasons, but is with large biases in vegetation seasons. The result is reasonable because this approach does not take the stomatal control into account, which may cause errors in vegetation seasons.

We attribute the difference of diurnal pattern between EF and ET_rF to the stomatal control, which is quantified as stomatal resistance (r_s). The direct measurement or the robust estimation of r_s are difficult, but the r_s has an robust correlation with the canopy resistance (r_c) excluded the effect of other factors such as vapor pressure deficiency (VPD), wind speed and soil evapo-

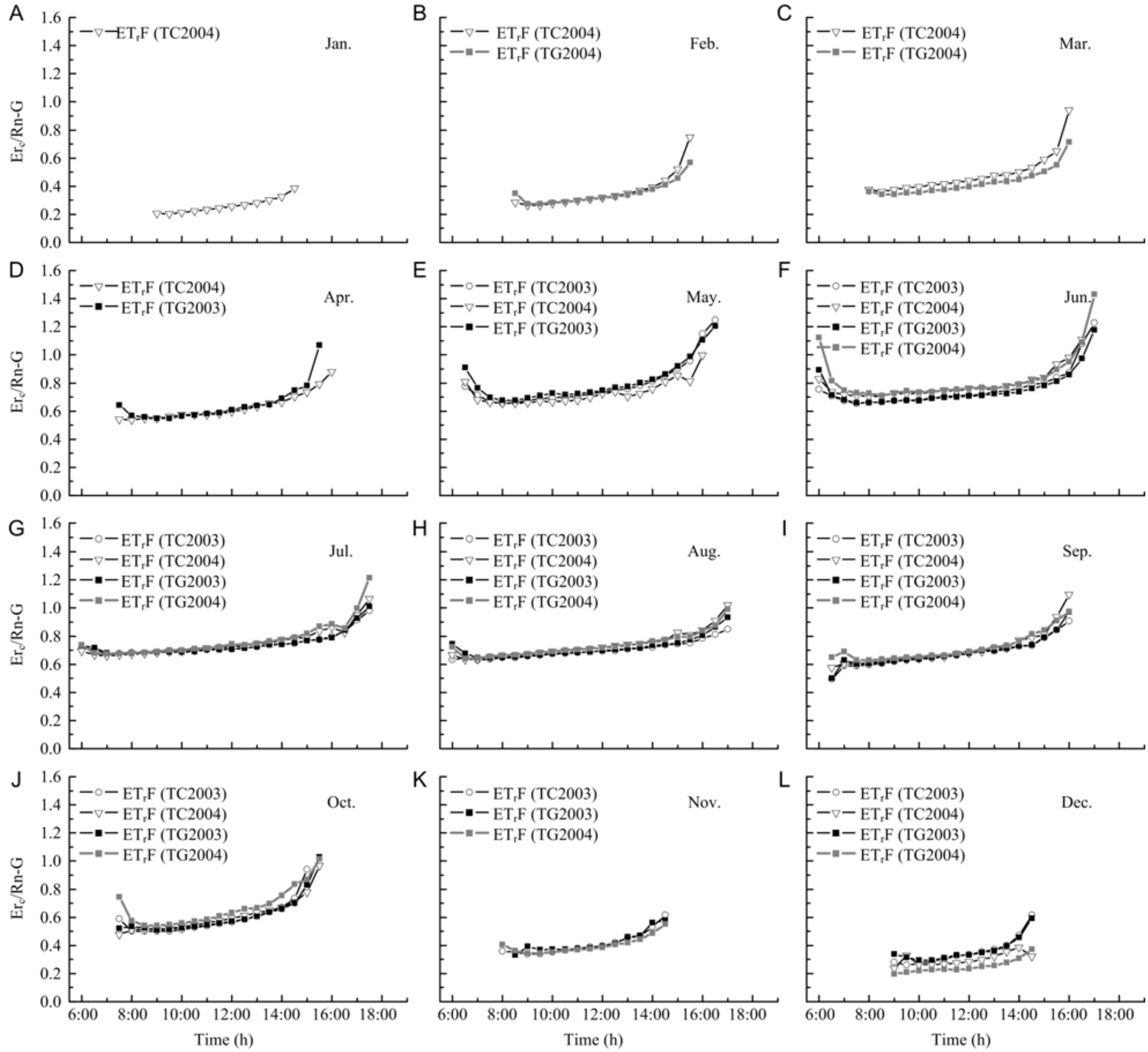

Fig. 6 Monthly mean value of the ratio of ET$_r$F diurnal pattern in region 2. TC, Tongyu crop land site; TG, Tongyu grass land site.

ration (Irmak *et al*. 2008), so the stomatal control can be reflected by the variance of r_c. However, the direct observation of r_c is unavailable in our study, so we speculate the possible diurnal pattern of r_c by analyzing the diurnal pattern of meteorological variables which are strongly relevant to r_c. According to Irmak and Mutiibwa (2010), the prominent relevant variables of r_c are the leaf area index (LAI), air temperature (T_a), net radiation (R_n), and VPD, which are either with high correlation coefficient and definite trend; as well as relative humidity (RH), with lower deterministic coefficient but clear trend. The LAI has the most prominent relationship with r_c, but the response of r_c to LAI appears at the seasonal scale rather than at the diurnal scale. Responded by R_n, the r_c should decrease in the afternoon, due to the large magnitude of stomatal closure at lower R_n; however, it is possible that r_c does not respond to the changes in R_n due to the control of r_c by other microclimatological variables. General trend of decreasing r_c with increasing T_a and *VPD* is reported, while the increasing RH will cause the increasing r_c.

The diurnal patterns of T_a, VPD and RH in the vegetation growing seasons in the two regions are presented in Figs. 7-9. The mean value of the whole vigorous growing season (i.e., March to May for wheat and July to September for maize in region 1, and June to September in region 2) is used. The T_a rises persistently before noon, and the increasing rate slows down after 12:00 a.m. The peak point happens three hours after the high noon, and after that, the T_a decreases slightly after that, but still remains at the high magnitude. Although the interannual variance of T_a is large in region 2 due to the large difference of precipitation in region 2, the pattern is similar (Fig. 7-C). The results showed that, despite the magnitude of T_a varies from different site, the diurnal pattern is similar regardless of the precipitation. Since T_a has a negative relation to r_c, the diurnal pattern of T_a implies that the r_c might be high in the morning, and decreases to a lower magnitude in the afternoon. The VPD has the same diurnal pattern as the T_a, with the maximum value comes around 3:00 p.m. Same pattern was also reported by Barton *et al*. (2010), and he also confirmed that r_c will decrease with the increase of VPD because the VPD is also negative related to r_c. The RH has the opposite trend with T_a and VPD, but the RH is positive related to r_c according to Imark and Mutiibwa's results (Imark and Mutiibwa 2010), which also adds weight to the assumption that r_c decreases in the day. Similar pattern was also found in other researches. Farah *et al*. (2004) proposed that EF was influenced by RH, T_a and VPD over woodland and grassland. Chehbouni *et al*. (2008) pointed out that RH is one of the most important factors influencing EF over olive orchard land.

The mechanism of the stomata is complicated because many factors can cause the changes in r_s. However, according to the analysis of meteorological variables having strong relationships with r_c and the difference between the diurnal pattern of EF and ET_rF, the assumption that the stomata tend to restrain the

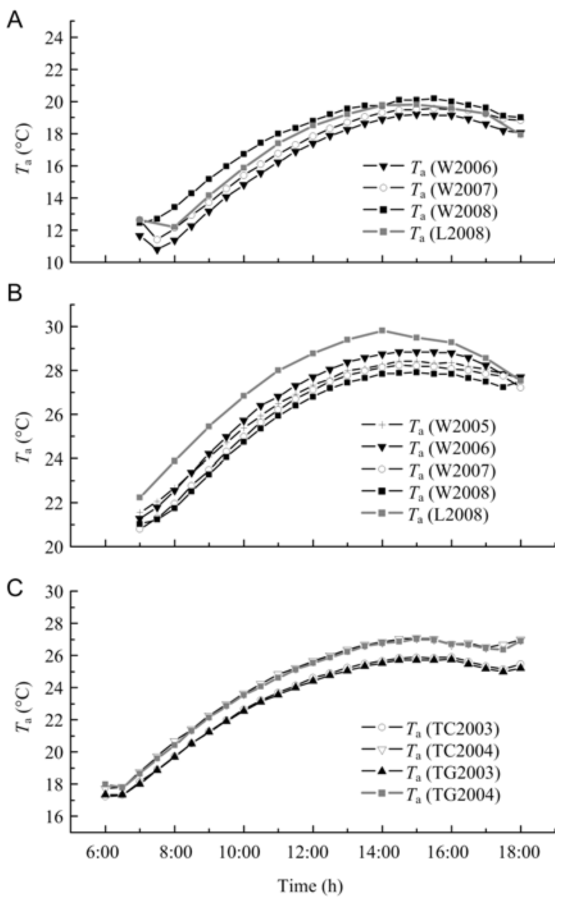

Fig. 7 Mean value of T_a diurnal pattern at different sites. A, Wheat growing seasons in region 1. B, maize growing seasons in region 1. C, wet seasons in region 2.

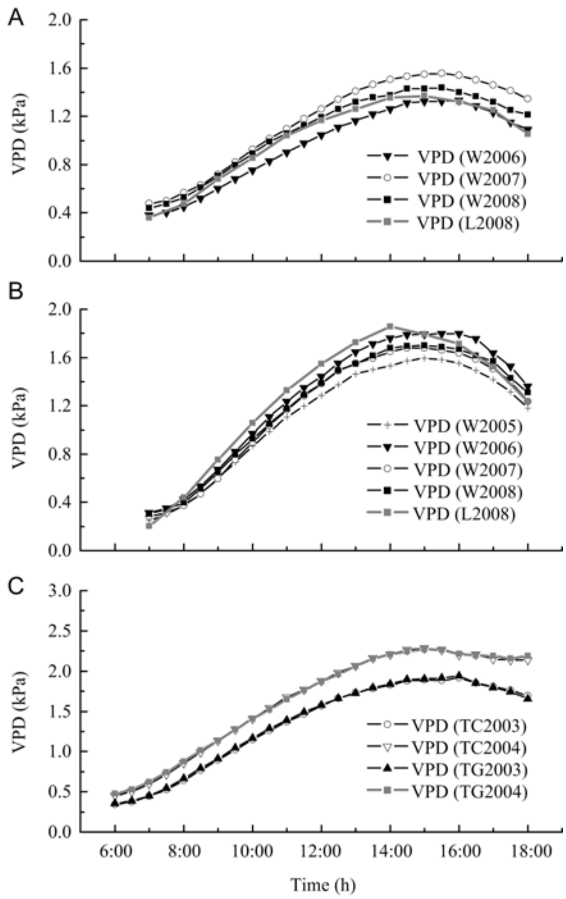

Fig. 8 Mean value of VPD diurnal pattern at different sites. A, wheat growing seasons in region 1. B, maize growing seasons in region 1. C, wet seasons in region 2.

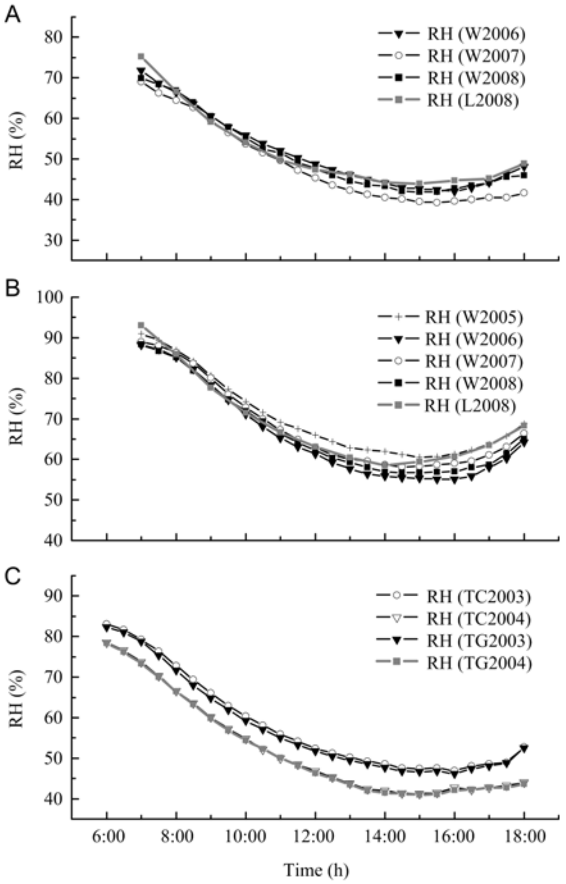

Fig. 9 Mean value of RH diurnal pattern at different sites. A, wheat growing seasons in region 1. B, maize growing seasons in region 1. C, wet seasons in region 2.

transpiration in the morning and promote it in the afternoon is confirmed in the two aspects.

CONCLUSION

This study is aimed at analyzing and providing insights into general diurnal pattern of EF over croplands and grassland under variant climate conditions, namely semi-humid and semi-arid regions. The long term continuous observations of flux at different sites show a drastic different pattern of EF in vegetation growing seasons, as the EF being the lowest at sunrise hour and increasing persistently throughout the daytime with a sharp increase a couple of hours before sunset. However, in non-vegetation seasons, the EF diurnal behavior shows a concave-up shape with a relatively constant EF in the most daytime period. Furthermore, the EF diurnal behavior is strongly dependent on soil water content and fractional coverage. Specifically as this: the larger fractional coverage excluded the soil water stress, the sharper increasing of EF diurnal pattern shows. Further analysis of ET_rF diurnal pattern dependencies shows that ET_rF diurnal pattern has a gentle and nearly constant behavior, which indicates that the weather effects have little influence on the behavior of EF diurnal pattern. We assume the discrepancy between EF and ET_rF diurnal pattern is due to the stomatal regulation. The diurnal pattern of air temperature, VPD, and relative humidity, which has strong effect on stomatal resistance, confirms this assumption. According to the EF diurnal behavior, the EF self-preservation method in extrapolating instantaneous LE into daily ET may not valid under certain condition, as the different over-passing time of various satellites can lead to absolutely different results and the method is no longer robust and universally applicable.

MATERIALS AND METHODS

Site description

The study takes place in two regions in the northern China, North China Plain (region 1) and Northeast China Plain (region 2), respectively (Fig. 10). Region 1 has two flux sites, the Weishan flux site and the Luancheng flux site. The predominant crops on both sites are winter wheat and summer maize which were planted in rotation. The growing season of winter wheat runs from mid-October to the following late May, while that for maize is from late June to early October. Region 2 has Tongyu Long-Term Land Surface Processes Observational Station, which is one of the reference sites of the Coordinated Energy and Water Cycle Observation Project (new CEOP, www.ceop.net). The station has two observation sites located on the cropland surface and degraded grassland surface, separately. The main crop is maize mixed with sunflower cultivated from May to late September on the cropland surface; while in the remaining months, the land cover is bare soil. On the degraded grassland, the maximum height of the grass is 10 cm during the growing seasons (June to September), but in winter, the height becomes less than 5 cm. Both of the two regions have a temperate continental monsoon climate with four distinct seasons, and 70-80% of the annual precipitation confine to the summer (June to August). The farming system of croplands on Tongyu site is bringing in one harvest a year, same as the other area in the Northeast China Plain, which has regional representative in this region. The difference is that region 1 belongs to a semi-humid climate zone with irrigation in wheat growing

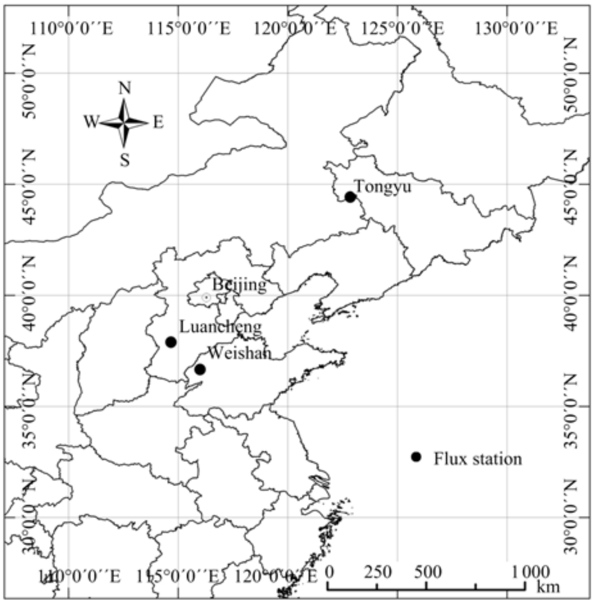

Fig. 10 Site locations.

seasons, while region 2 belongs to a semi-arid climate zone and the lack of irrigation leads to a severe deficit of water. The two regions are selected because wheat and maize are major grain production of China, which account for 26 and 22% of the total areas and 21 and 26% of the total food production of China, respectively (Minstry of Agriculture, China 1999). Table 1 lists site descriptions, and more details of the site information are available in the literature (Shen *et al*. 2004; Liu *et al*. 2008; Lei and Yang 2010a).

Field measurements and data acquisition

Each of the four sites has an eddy covariance (EC) system to measure sensible heat flux and latent heat flux. Flux data in Weishan site are corrected for coordinate rotation, spectral loss, density fluctuations, and sonic virtual temperature conversion by Lei and Yang (2010b). Fluxes in Luancheng are also adjusted for variations in air density due to the transfer of water vapor and sensible heat. The quality control is made in Tongyu site by using CEOP data Quality Control Interface System (QC-IF) (http://ceop-qc.tkl.iis.u-tokyo.ac.jp/QC/CEOP.html). Although inevitably energy unbalance around 20% is found in the EC system, the systematical error does not have a great effect on the diurnal pattern of EF. In order to avoid the impact of extra uncertainties in the process of enforcing energy balance closure, direct observations of the EC system are used in this study. Downward/upward solar and longwave radiations are measured separately and net radiation is then calculated. Soil heat flux is determined by averaging measurement profiles obtained near the flux sites, two for Weishan and Tongyu, and three for Luancheng. Volumetric soil water content is measured at the four sites at different depths with a neutron probe. Detailed flux measurements as well as meteorological parameters, including air temperature, relative humidity, wind speed and precipitation, are listed in Table 2. For Luancheng site, meteorological parameters are obtained from the station of the Chinese Ecological Research Network which stands the same place as the flux site.

Normalized differential vegetation index (NDVI) data are used for the analysis of the vegetation cover condition. NDVI from the grids containing the flux sites during the study period are calculated from MODIS/Terra 8-day composite reflectance product (MOD09Q1) for the red and near infrared bands with a 250 m resolution, downloaded from the NASA Data Center (http://reverb.echo.nasa.gov/reverb/).

Data processing

Before assessing the EF diurnal pattern using the EC data, a data processing procedure is made to eliminate bad quality flux data. The self-preservation assumption is applied to daytime fluxes under fair weather conditions, so fluxes

Table 1 Site descriptions

Sites	Weishan	Luancheng	Tongyu
Coordinates	116°03′E, 36°39′N	114°41′E, 37°53′N	122°52′E, 44°25′N
Elevation	30 m a.s.l.	50 m a.s.l.	184 m a.s.l.
Soil type	Silt loam	Loamy soil	Sandy loam
Mean annual temperature	13.8°C[1)]	12.8°C[3)]	5.7°C[6)]
Mean annual precipitation	553 mm[1)]	485 mm[3)]	388 mm[6)]
Mean annual pan evaporation (Φ 20)	1 950 mm[2)]	1 616 mm[4)]	1 879 mm[4)]
Mean annual irrigation	215 mm[1)]	300-400 mm[5)]	No irrigation
Available data periods	2005.5-2008.12	2007.11-2008.9	2002.10-2004.12

[1)] The values are the averages from 1990 to 2008.
[2)] The values are the averages from 1961 to 2005.
[3)] The values are the averages from 1960 to 2003.
[4)] The values are the averages from 1955 to 2001.
[5)] The data is quoted from literatures (Lei and Yang 2010; Shen *et al*. 2004).
[6)] The values are the averages from 1971 to 2000.

Table 2 Detailed introductions of *in situ* measurements of four sites

Site	Parameters	Instruments	Height/Depth[1)]	Interval
Weishan	Sensible/latent heat flux	CSAT3, LI7500, Campbell Scientific, Inc., Logan, UT, USA	3.7 m	30 min
	Downward/upward solar/longwave radiations	CNR-1, Kipp & Zonen, Delft, the Netherlands	3.5 m	10 min
	Soil heat flux	HFP01SC, Hukseflux, Delft, the Netherlands	-0.03 m	10 min
	Soil water content	TRIME-EZ/IT, IMKO, Ettlingen, Germany	-0.05/0.1/0.2 m	10 min
	Air temperature and relative humidity	HMP45C, Vaisala Inc., Helsinki, Finland	3.6 m	10 min
	Air pressure	Druck-CS115, Campbell Scientific, Inc., Logan, UT, USA	2.0 m	10 min
	Wind speed	05103, Young Co., 120 Traverse City, MI, USA	10.0 m	10 min
	Precipitation	TE525MM, Campbell Scientific Inc., 121 Logan, UT, USA	1.5 m	10 min
Luancheng	Sensible/latent heat flux	CSAT3, LI7500 Campbell Scientific, Inc., Logan, UT, USA	3.3 m	1 h
	Downward/upward solar/longwave radiations	CNR-1, Kipp & Zonen, Delft, the Netherlands	3.0 m	1 h
	Soil heat flux	HFP01, Hukseflux, Delft, the Netherlands	-0.02 m	1 h
Tongyu	Sensible/latent heat flux	CSAT3, LI7500, Campbell Scientific, Inc., Logan, UT, USA	3.5 m || 2.0 m[2)]	30 min
	Downward/upward solar/longwave radiations	CM21, Kipp & Zonen, Delft, the Netherlands	3.0 m || 2.0 m[2)]	30 min
	Soil hear flux	HFP01SC_L50, Hukseflux, Delft, the Netherlands	-0.05/-0.10 m	30 min
	Soil water content	CS616_L, Campbell Scientific, Inc., Logan, UT, USA	-0.05/0.1/0.2 m || -0.05/0.1 m[2)]	30 min
	Air temperature	HMP, Vaisala Inc., Helsinki, Finland	1.95 m || 1.35 m[2)]	30 min
	Specific humidity	45C_L, Vaisala Inc., Helsinki, Finland	1.95 m || 1.35 m[2)]	30 min
	Air pressure	CS105, Texas Electronics, Inc., Dallas, TX, USA	1.5 m	30 min
	Wind speed	034A_L, Met One Instruments, Inc., Rowlett, TX, USA	17.06 m || 17.46 m[2)]	30 min
	Precipitation	TE525MM_L, Texas Electronics, Inc., Dallas, TX, USA	1.0 m	30 min

[1)] The minus sign means measurements below ground.
[2)] The left is for cropland site and the right is for grassland site.

in precipitation days are eliminated. The present study takes palace in different regions and covered all seasons, and the sunrise hour and the sunset hour might differ greatly. A variable timer line is used as we defined the daytime is the period when shortwave solar radiation is above 20 W m^{-2}. Then, we eliminate the EF data which are out of the reasonable range proposed by Brotzge and Crawford (2003). Finally, a month-by-month spike detection is made. Specifically as this: any value that exceeds the mean value ±2.5 times the standard deviation in a window of a month is labeled as spike (Mauder *et al*. 2006), looping until all the spikes are found out.

Fractional coverage (f_c) is used in this study to analyze the vegetation cover condition, which can be estimated from NDVI, as:

$$f_c=\frac{NDVI\text{-}NDVI_{\min}}{NDVI_{\max}\text{-}NDVI_{\min}} \quad (1)$$

Where $NDVI_{max}$ and $NDVI_{min}$ are *NDVI*s with 98% and 5% distributions, respectively. Suggested $NDVI_{max}$ for wheat (also grass) and maize are 0.7909 and 0.7859, respectively, and that for $NDVI_{min}$ is 0.051 for both wheat and maize (Lokupitiya *et al*. 2009). The NDVI data are preprocessed with the quality flags in the dataset to remove the cloud contaminant images. A twice filter smoothing algorithm is used to reduce the noise in the NDVI time series (Velleman 1980).

Method for analyzing EF diurnal pattern

Reference evapotranspiration (ET_r) associated with the crop coefficient (K_c) is one of the most widely known and employed ways for estimating consumptive use of water. The actual crop *ET* is thus estimated using ET_r multiplied by K_c as:

$$ET=K_cET_r \quad (2)$$

In general, there are three primary characteristics in distinguish actual *ET* from ET_r: (i) the reflectance of the vegetation and soil surface to the radiation; (ii) aerodynamic roughness of the vegetation; and (iii) resistance within the vegetation canopy and soil surface in heat and momentum transfer. In the analysis of the diurnal pattern of *EF*, the first characteristic can be omitted because the *EF* is the ratio between *ET* and the radiation. The other two characteristics can be represented by ET_r and K_c, respectively, because ET_r represents nearly all effects of weather, and K_c varies predominately with specific crop characteristics and only a small amount with climate (Allen *et al*. 2005). In this study, we choose the reference evaporative fraction (ET_rF), defined as the ratio between ET_r and available energy ($ET_rF=ET_r/(R_n\text{-}G)$), and the K_c as two major dependencies of the diurnal pattern of EF. However, K_c is an empirical coefficient which cannot be measured directly, so we use vegetation fraction and vegetation stomatal regulation instead. These variables have strong relationship with K_c. Here, we use ET_r calculated by the following equation recommended by Allen *et al*. (1998):

$$ET_r=\frac{0.408\Delta(R_n\text{-}G)+\gamma\dfrac{900}{T_a+273}u_2(e_s\text{-}e_a)}{\Delta+\gamma(1+0.34u_2)} \quad (3)$$

Where ET_r is in the unit of mm d^{-1}, R_n and G are net radiation and soil heat flux, respectively (MJ m^{-2} d^{-1}), T_a is the air temperature (°C), u_2 is the wind speed at 2 m height (m s^{-1}), e_s-e_a is the saturation vapor pressure deficit (kPa), Δ is the slope vapor pressure curve (kPa/°C), and γ is the psychrometric constant (kPa/°C). All these parameters can be calculated from the meteorological measurements.

Acknowledgements

This research was supported by the the National Natural Science Funds for Distinguished Yong Scholar, China (51025931) and the National Natural Science Foundation of China (50939004). The author would like to thank Coordinated Energy and Water Cycle Observation Project (CEOP) distributed by CEOP Data Archive for providing the flux data from Tongyu site.

References

Allen R G, Pereira L S, Raes D, Smith M. 1998. Crop evapotranspiration: guidelines for computing crop requirements. In: *Irrigation and Drainage Paper No. 56*. FAO, Rome, Italy.

Allen R G, Pereira L S, Smith M, Wright J. 2005. FAO-56 dual crop coefficient method for estimating evaporation from soil and application extensions. *Journal of Irrigation and Drainage Engineering-ASCE*, **131**, 2-13.

Allen R G, Tasumi M, Trezza R. 2007. Satellite-based energy balance for mapping evapotranspiration with internalized calibration (METRIC)-model. *Journal of Irrigation and Drainage Engineering-ASCE*, **133**, 380-394.

Barton C V M, Ellsworth D S, Medlyn B E. 2010. Whole-tree chambers for elevated atmospheric CO_2 experimentation and tree scale flux measurements in south-eastern Australia: the hawkesbury forest experiment. *Agricultural and Forest Meteorology*, **150**, 941-951.

Bastiaanssen W G M, Menenti M, Feddes M F, Holtslag A A M. 1998. A remote sensing surface energy balance algorithm for land (SEBAL): 1. Formulation. *Journal of Hydrology*, **212-213**, 198-212.

Brotzge J A, Crawford K C. 2003. Examination of the surface energy budget: A comparison of eddy correlation and Bowen ratio measurement systems. *Journal of Hydrometeorology*, **4**, 160-178.

Brutsaert W, Sugita M. 1992. Application of self-preservation in the diurnal evolution of the surface energy budget to determine daily evaporation. *Journal of Geophysical Research*, **97**, 18377-18382.

Burba G G, Verma S B. 2005. Seasonal and interannual variability in evapotranspiration of native tallgrass prairie and cultivated wheat ecosystems. *Agricultural and Forest Meteorology*, **135**, 190-201.

Caparrini F, Castelli F, Entekhabi D. 2004. Estimation of surface turbulent fluxes through assimilation of radiometric surface temperature sequences. *Journal of Hydrometeorology*, **5**, 145-159.

Chehbouni A, Hoedjes J C B, Rodriquez J C, Watts C J, Caratuza J, Jacob F, Kerr Y H. 2008. Using remotely sensed data to estimate area-averaged daily surface fluxes over a semi-arid mixed agricultural land. *Agricultural and Forest Meteorology*, **148**, 330-342.

Ministry of Agricultur, China. 2009. *China Agricultural Yearbook*. China Agriculture Press, Beijing. p. 247. (in Chinese)

Crago R D. 1996. Conservation and variability of the evaporative fraction during the daytime. *Journal of Hydrology*, **180**, 173-194.

Crago R D, Brutsaert W. 1996. Daytime evaporation and the self-preservation of the evaporative fraction and the Bowen ratio. *Journal of Hydrology*, **178**, 241-255.

Farah H O, Bastiaanssen W G M, Fedders R A. 2004. Evaluation of the temporal variability of the evaporative fraction in a tropical watershed. *International Journal of Applied Earth Observation and Geoinformation*, **5**, 129-140.

Gentine P, Entekhabi D, Chehbouni A, Boulet G, Duchemin B. 2007. Analysis of evaporative fraction diurnal behavior. *Agricultural and Forest Meteorology*, **143**, 13-29.

Hoedjes J C B, Chehbouni A, Jacob F. 2008. Deriving daily evapotranspiration from remotely sensed instantaneous evaporative fraction over olive orchard in semi-arid Morocco. *Journal of Hydrology*, **354**, 53-64.

Irmak S, Mutiibwa D. 2010. On the dynamics of canopy resistance: Generalized-linear estimation and relationships with primary micrometeorological variables. *Water Resources Research*, **46**, W08526.

Irmak S, Mutiibwa D, Irmak A, Arkebauer T J, Martin D L, Eisenhauer D E. 2008. On the scaling up leaf stomatal resistance to canopy resistance using photosynthetic photon flux density. *Agricultural and Forest Meteorology*, **148**, 1034-1044.

Jackson R D, Hatfield J L, Reginato RJ, Idso S B, Pinter Jr P J. 1983. Estimation of daily evapotranspiration from one time-of-day measurements. *Agricultural Water Management*, **7**, 351-362.

Kustas W P, Schmugge T J, Humes K S, Jackson T J, Parry R, Weltz M A, Moran M S. 1993. Relationships between evaporative fraction and remotely-sensed vegetation index and microwave brightness temperature for semiarid rangelands. *Journal of Applied Meteorology*, **32**, 1781-1790.

Kustas W P, Li F, Jacson T J, Prueger J H, MacPherson J I, Wolde M. 2004. Effects of remote sensing pixel resolution on modeled energy flux variability of croplands in Iowa. *Remote Sensing of Environment*, **92**, 535-547.

Lei H, Yang D. 2010a. Interannual and seasonal variability in evapotranspiration and energy partitioning over an irrigated cropland in the North China Plain. *Agricultural and Forest Meteorology*, **150**, 581-589.

Lei H, Yang D. 2010b. Seasonal and interannual variations in carbon dioxide exchange over a cropland in the North China Plain. *Global Change Biology*, **16**, 2944-2957.

Lhomme J P, Elguero E. 1999. Examination of evaporative fraction diurnal behaviour using a soil-vegetation model coupled with a mixed-layer model. *Hydrology and Earth*

System Sciences, **3**, 259-270.

Li S, Kang S Z, Li F S. 2008. Vineyard evaporative fraction based on eddy covariance in an and desert region of Northwest China. *Agricultural Water Management*, **95**, 937-948.

Li S G, Eugster W, Asanuma J, Kotani A, Davaa G, Oyunbaatar D, Sugita M. 2006. Energy partitioning and its biophysical controls above a grazing steppe in central Mongolia. *Agricultural and Forest Meteorology*, **137**, 89-106.

Li Z L, Tang R, Wan Z, Bi Y, Zhou C, Tang B, Yan G, Zhang X. 2009. A review of current methodologies for regional evapotranspiration estimation from remotely sensed data. *Sensors*, **9**, 3801-3853.

Liu C M, Zhang X Y, Zhang Y Q. 2002. Determination of daily evaporation and evapotranspiration of winter wheat and maize by large-scale weighing lysimeter and micro-lysimeter. *Agricultural and Forest Meteorology*, **111**, 109-120.

Liu H Z, Tu G, Dong W J. 2008. Three-year changes of surface albedo of degraded grassland and cropland surfaces in a semiarid area. *Chinese Science Bulletin*, **53**, 1246-1254.

Lokupitiya E, Denning S, Paustian K, Baker I, Schaefer K, Verma S, Meyers T, Bernacchi C J, Suyker A, Fischer M. 2009. Incorporation of crop phenology in simple biosphere model (SiBcrop) to improve land-atmosphere carbon exchanges from croplands. *Biogeosciences*, **6**, 969-986.

Mauder M, Liebethal C, Gockede M, Leps J P, Beyrich F, Foken T. 2006. Processing and quality control of flux data during LITFASS-2003. *Boundary-Layer Meteorology*, **121**, 67-88.

Nichols W E, Cuenca R H. 1993. Evaluation of the evaporative fraction for parameterization of the surface energy balance. *Water Resources Research*, **29**, 3681-3690.

Sànchez J M, Kustas W P, Caselles V, Anderson M C. 2008. Modelling surface energy fluxes over maize using a two-source patch model and radiometric soil and canopy temperature observations. *Remote Sensing of Environment*, **112**, 1130-1143.

Shen Y J, Zhang Y Q, Kondoh A, Tang C, Chen J, Xiao J, Sakura Y, Liu C, Sun H. 2004. Seasonal variation of energy partitioning in irrigated lands. *Hydrological Processes*, **18**, 2223-2234.

Shuttleworth W J, Gurney R J, Hsu A Y, Ormsby J P. 1989. FIFE: the variation in energy partition at surface flux sites. Remote sensing and large-scale global processes. *IAHS Publication*, **186**, 67-74.

Su Z. 2002. The surface energy balance system (SEBS) for estimation of turbulent heat fluxes. *Hydrology and Earth System Sciences*, **6**, 85-99.

Stewart J B. 1996. Extrapolation of evaporation at time of satellite overpass to daily totals. In: Stewart J B, Engman E T, Feddes R A, Kerr Y, eds., *Scaling up in Hydrology Using Remote Sensing*. Wiley, Chichester, UK.

Sugita M, Brutsaert W. 1991. Daily evaporation over a region from lower boundary layer profiles measured with radiosondes. *Water Resources Research*, **27**, 747-752.

Suleiman A, Crago R. 2004. Hourly and daytime evapotranspiration from grassland using radiometric surface temperatures. *Agronomy Journal*, **96**, 384-390.

Trezza R. 2002. Evapotranspiration using a satellite-based surface energy balance with standardized ground control. Ph D thesis, Utah State University, Logan, UT. p. 339.

Velleman P. 1980. Definition and comparison of robust nonlinear data smoothing algorithms. *Journal of the American Statistical Association*, **75**, 609-615.

Yang D, Li C, Hu H, Lei Z, Yang S, Kusuda T, Koike T, Musiake K. 2004. Analysis of water resources variability in the Yellow River of China during the last half century using historical data. *Water Resources Research*, **40**, W06502.

Zhang L, Lemeur R. 1995. Evaluation of daily evapotranspiration estimates from instantaneous measurements. *Agricultural and Forest Meteorology*, **74**, 139-154.

(Managing editor SUN Lu-juan)